Local Properties at Interfaces in Nanodielectrics: An *ab initio* Computational Study

Ning Shi and **Ramamurthy Ramprasad**
Institute of Materials Science
Department of Chemical, Materials, and Biomolecular Engineering
University of Connecticut
Storrs, CT 06269, USA

ABSTRACT

First-principles computational methodologies are presented to study the impact of surfaces and interfaces on the dielectric and electronic properties of emerging technologically important systems over length scales of the order of inter-atomic distances. The variation of dielectric constant across Si-SiO$_2$, Si-HfO$_2$ and SiO$_2$-polymer interfaces has been correlated to interfacial chemical bonding environments, using the theory of the local dielectric permittivity. The local electronic structure variation across Si-HfO$_2$ and SiO$_2$-polymer interfaces, including band bending, band offsets and the creation of interfacial trap states have been investigated using a layer-decomposed density of states analysis. These computational methods form the groundwork for a more thorough analysis of the impact of surfaces, interfaces, and atomic level defects on dielectric and electronic properties of a wide variety of nano-structured systems.

Index Terms — **Dielectric films, dielectric polarization, interface phenomena, density functional theory, electronic structure.**

1 INTRODUCTION

IN recent years, dielectric materials of nanoscale dimensions have aroused considerable interest. We mention two examples. First, in the semiconductor industry, in order to keep pace with Moore's law scaling, the thickness of the gate oxide dielectric material is reaching nanoscale dimensions [1, 2]. Second, the high energy density capacitor industry is currently considering dielectric composites with a polymer host matrix filled with inorganic dielectric nanoparticles [3-7] or polarizable organic molecules [8]. The driving force for the former application is high dielectric constants (or high-k), and those for the latter are high-k and/or high dielectric breakdown strengths.

As component sizes or dimensions in multiple-component systems shrink to the atomic or nanoscale, the structure and chemistry at interfaces become important and can sometimes dominate the overall properties. For instance, while atomic level interfacial features such as dangling bonds, under- or over-coordination, multiple-oxidation states, impurities, etc., may be less important in larger scale systems owing to the smaller volume fraction occupied by the interfacial region, the consequences of such effects especially on electrical properties can reach unanticipated magnitudes in nanoscale systems [9-12].

Thus, it is important to characterize the electronic and dielectric properties of interface-containing materials in the nano-regime.

The present investigation constitutes an initial step towards such a fundamental understanding of the relationship between interface structure and chemistry on the one hand, and properties such as interfacial polarization, dielectric response, and electronic structure on the other. Specifically, (i) the extent to which surface/interface effects modify the static and optical *local* dielectric permittivity, and (ii) the evolution of the *local* electronic structure (e.g., the valence and conduction bands) across interfaces as a function of position are addressed using *ab initio* density functional theory based computational methods. Two critical classes of systems are considered in this work. These include interfaces between Si and the inorganic oxides SiO$_2$ or HfO$_2$, targeting the first application example mentioned above, and interfaces between model polymers (polyethylene or polyvinylidene difluoride) and SiO$_2$, relevant for the second application example.

This manuscript is organized as follows. Section 2 discusses the technical details of our computational approach. In Section 3, we describe our theory of the local permittivity, and its application to Si-SiO$_2$, Si-HfO$_2$ and SiO$_2$-polymer interfaces. The local electronic structure across those interfaces is then discussed in Section 4, in terms of the layer-decomposed density of states. We finally conclude with a summary in Section 5.

2 METHODS AND MODELS

Density functional theory (DFT) offers an efficient, accurate and fundamental route to the *ab initio* numerical computation of electronic, atomic, molecular and solid-state properties [13]. Below, we provide details concern-ing the specific implementation and approximations of DFT as used in the present work.

All calculations were performed using the local density approximation (LDA) within DFT [13] as implemented in the local orbital SIESTA code [14]. Within this implementation, the electronic wave functions are expanded using a double-zeta plus polarization basis set. Electron-ion interactions were represented using norm-conserving non-local pseudopotentials of the Troullier–Martins type, one for each element. The atomic configurations of $[Kr4d^{10}4f^{14}5s^25p^6]5d^26s^2$, $[Ne]3s^23p^2$, $[He]2s^22p^5$, $[He]2s^22p^4$, $[He]2s^22p^2$, and $[H]$ were used for Hf, Si, F, O, C, and H pesudopotentials, respectively. Semi-core corrections were used for Hf and Si. Integration of properties over the first Brillouin zone was performed via the Monkhorst-Pack k point sampling scheme. 75 special k points yielded well converged bulk results for Si. The numbers of k points used for the bulk SiO_2 in α-quartz and β-cristobalite phases were 108 and 74, respectively, and those for bulk HfO_2 in the cubic and tetragonal phases were 75 and 112. In the case of slab systems containing Si-SiO_2 and Si-HfO_2 interfaces, 64 and 36 special k points were required, respectively, to result in well converged results. For the SiO_2-polymer interfaces considered here, namely, polyethylene (PE) on SiO_2 in the α-quartz phase and polyvinylidene difluoride (PVDF) on SiO_2 in the β-cristobalite phase, 18 special k points were used. The equilibrium positions of the atoms in all cases were determined by requiring the forces on each atom to be smaller than 0.01 eV/Å.

The computed structural parameters for the model systems described above are listed, and compared with other DFT work and experiments, in Table I. The equilibrium lattice constant of Si in the diamond crystal structure was calculated here to be 5.43 Å, which agrees well with prior DFT calculations [15, 16] and experiments [17]. The equilibrium lattice constants, *a* and *c*, in α-quartz SiO_2 calculated to be 4.91 Å and 5.41 Å, respectively, also agree well with prior DFT calculations [18, 19] and with experimental results [20]. For SiO_2 in the β-cristobalite phase, the calculated lattice constant was 7.49 Å, in reasonable agreement with other theory [21] and experiments [22]. The equilibrium lattice constant of cubic HfO_2 was calculated to be 5.02 Å, and the *a* and *c* equilibrium lattice constants of tetragonal HfO_2 were calculated to be 4.99Å and 5.06 Å, respectively, all in good agreement with prior DFT calculations [23,24] and experiments [25,26]. A $C_{12}H_{26}$ hydrocarbon chain and a $C_6F_7H_7$ chain were used to model PE and PVDF, respectively. As can be seen from Table I, calculated bond lengths in these chains are in good agreement with prior calculations [27, 29, 30] and experiments [28].

Table 1. Comparison of calculated structural parameters of bulk Si, SiO_2, HfO_2, PE, PVDF, and vinlysilanediol with literature values. All distances are in Å.

System	Lattice constant/ bond length	This work	Other DFT	Expt.
Si	a	5.43	5.48[a]	5.43[b]
SiO_2 (α-quartz)	a	4.91	5.02[c]	4.92[d]
	c	5.41	5.53[c]	5.41[d]
SiO_2 (β-cristobalite)	a	7.49	7.14[e]	7.17[f]
HfO_2 (Cubic)	a	5.02	5.04[h]	5.08[i]
HfO_2 (Tetragonal)	a	4.99	5.06[h]	5.14[i]
	c	5.06	5.12[h]	5.25[i]
PE	C-C	1.51	1.54[j]	1.54[k]
	C-H	1.12	1.10[j]	1.10[k]
PVDF	C-H	1.09	1.08[l]	1.10[k]
	C-F	1.36	1.37[l]	1.34[k]
	C=C	1.34	1.33[m]	1.34[k]
Vinylsilanediol	Si-C	1.83	1.87[m]	1.89[k]
	Si-H	1.51	1.48[m]	1.48[k]

[a] Reference 15,16; [b] Reference 17 ; [c] Reference 18,19; [d] reference 20; [e] Reference 21; [f] Reference 22; [h] Reference 23,24; [i] Reference 25,26; [j] Reference 27; [k] Reference 28; [l] Reference 29; [m] Reference 30.

3 THE *LOCAL* PERMITTIVITY

As mentioned in Section 1, owing to the fundamentally different chemistries at surfaces and interfaces compared to the bulk part of a material, the dielectric response is expected to be different in these regions. In fact, our recent work on the scaling with thickness of the dipole moment induced due to an external electric field in ultra-thin SiO_2 [31] and HfO_2 [32] slabs has resulted in the realization that the dielectric properties in the surface regions are considerably different from those of the bulk. This scaling analysis has resulted in an alternative method for the computation of both the static and optical *bulk* polarization and dielectric constant, considerably more efficient than conventional first principles methods [23, 33, 34] used to compute these quantities. Nevertheless, a quantitative estimation of the dielectric constant or polarization at surface and interface regions was not possible using this approach.

Below we present the theory of the *local*, or position-dependent, dielectric permittivity [35, 36], which when combined with DFT computations allows for the deter-mination of such interfacial dielectric response. We then apply this theory to a few important interface containing systems.

3.1 THEORY

The local microscopic dielectric polarization $\vec{p}(r)$ can be obtained from the field induced charge density $\rho_{ind}(r)$ through the in-medium Maxwell equation [37]:

$$\nabla \cdot \vec{p}(r) = -\rho_{ind}(r) \qquad (1)$$

In the case of multi-layered (1-dimensional) systems with the layers oriented along the *x-y* plane, such as those considered here, Equation (1) reduces to:

$$\frac{d}{dz}\overline{p}(z) = -\overline{\rho}_{ind}(z) \qquad (2)$$

where $\overline{p}(z)$ and $\overline{\rho}_{ind}(z)$ are the polarization and induced charge density along the z-axis, respectively, averaged along the x-y plane. The induced charge density $\overline{\rho}_{ind}(z)$ can be evaluated as the difference of the total charge densities due to positive ($+\delta$) and negative ($-\delta$) external electric fields along the z direction. In the present work, δ was chosen to be 0.01 V/Å. The solution of Equation (2) is the following:

$$\overline{p}(z) = \overline{p}_{-\infty} - \int_{-\infty}^{z} \overline{\rho}_{ind}(z')dz' \qquad (3)$$

For the case when our slab system is located about the $z = 0$ plane, the constant $\overline{p}_{-\infty}$ can be set to zero as it corresponds to the polarization at $-\infty$, a region where charge density is zero.

Using the above procedure, both the optical (high frequency) and the static (low frequency) microscopic polarization can be calculated, respectively, by either allowing just the electrons, or both the electrons and the atoms, to respond to the applied external electric field. The local permittivity profile can then be computed from the local polarization using:

$$\varepsilon(z) = \frac{\varepsilon_0 E_{ext}}{\varepsilon_0 E_{ext} - \overline{p}(z)} \qquad (4)$$

where $E_{ext} = 2\delta$.

The optical and static local permittivities can be obtained from $\overline{p}(z)$ corresponding to the optical and static cases, respectively [35, 36].

3.2 Si-SiO$_2$ AND Si-HfO$_2$ INTERFACES

Miniaturization of electronic devices has already lead to ultra-thin (2-3 nm) SiO$_2$ layers in today's metal-SiO$_2$-Si gate stacks [9, 38] In order to keep pace with the miniaturization trend as specified by Moore's law, the SiO$_2$ dielectric will soon be replaced by a high dielectric constant (high-k) metal oxide [1,2]. The leading contender for the high-k oxide is HfO$_2$ which has a dielectric constant of about 25, much higher than the SiO$_2$ dielectric constant of about 4.5. Although Hf-based oxides are thermo-dynamically stable on Si, they are not kinetically stable, and silicides, silicates and SiO$_x$ are known to form at the interface, which have a much lower dielectric constant than HfO$_2$ [43-46]. An understanding of the factors controlling the dielectric properties of the interface between the dielectric and other materials calls for an accurate determination of atomic-scale dielectric permittivity profiles across layered structures.

The Si-SiO$_2$ interface has been studied for many decades. We focus on this interface first before moving on to Si-HfO$_2$. We consider a coherent Si-SiO$_2$ interface consisting of crystalline Si and SiO$_2$, of thickness 10.96 Å and 14.70 Å, respectively, with the latter having the β-cristobalite structure.

Figure 1 shows the static and optical permittivity profile across a Si-SiO$_2$ interface as a function of position along the direction normal to the interface. The dielectric constants in the interior of SiO$_2$ and Si regions are in excellent agreement with experimental values of the corresponding bulk systems (static and optical values of about 12 for Si [39], and 4.5 and 2.5 for SiO$_2$ [40, 41], respectively). However, in the transition

region between Si and SiO$_2$ and close to the outer surface planes, we find an enhancement of the dielectric constant, compared to that of the bulk values. The deviation at the surface is due to the under-coordination of Si atoms, which renders these atoms more polarizable. The enhanced permittivity at the interface (on the SiO$_2$ side) is due to Si atoms in SiO$_2$ existing in multiple oxidation states (i.e., Si, Si^{+1}, Si^{+2} and Si^{+3}) [15, 16], and is in quantitative agreement with capacitance measurements performed on ultra-thin SiO$_2$ layers on Si [42].
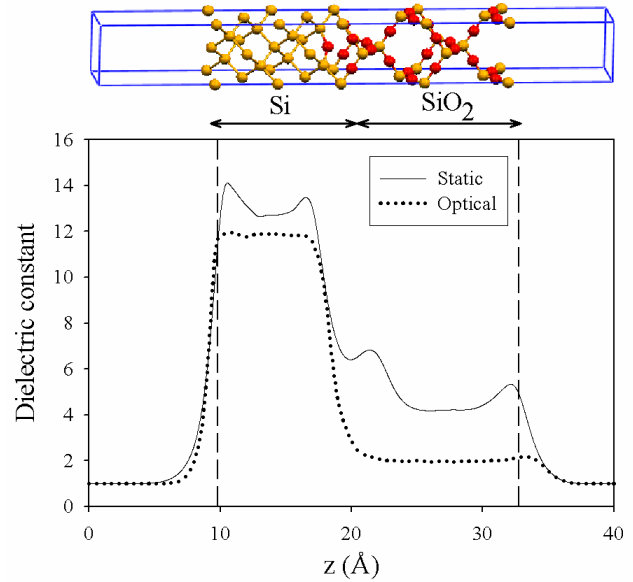
Figure 1. Above: Atomic model of Si-SiO$_2$ interface, with Si shown in gold, and O in red. In this and all other figures, the atomic model repeats periodically in the plane normal to the interface (x-y) plane. Below: Static (solid) and optical (dotted) dielectric constant of Si-SiO$_2$ stack as a function of position z normal to the interface.

The Si-HfO$_2$ interface is poorly understood due to its complicated interfacial structure, especially as new interfacial phases tend to form [43-46]. Here, we consider a simple model of expitaxial Si-HfO$_2$ primarily to demonstrate the local permittivity approach. Our model was created by placing an O-terminated (001) tetragonal HfO$_2$ slab on Si such that the HfO$_2$ slab was coherently matched on top of Si. The thickness of Si and HfO$_2$ layers were 10.95 Å and 19.91 Å, respectively. The resulting relaxed structure shows that half the interface O atoms move downwards towards Si, and the other half move upwards towards the Hf layer, as shown in Figure 2, thereby forming Si-O-Si and Hf-O-Hf bonds passivating *all* interfacial Si and Hf atoms.

The position-dependent dielectric constant along the Si-HfO$_2$ interface normal is shown in Figure 2. The dielectric constants in the interior of the HfO$_2$ and Si regions again match well with the corresponding experimental bulk values (the static and optical permittivities of tetragonal HfO$_2$ are 16 and 5, respectively [23, 33, 47]). As in the Si-SiO$_2$ case, enhancement of the permittivities at the free surfaces compared to the corresponding bulk values can be seen here as well, again due to under-coordination of surface atoms. However, in marked contrast with the Si-SiO$_2$ case, a *decrease* in the permittivity values results in the Si-HfO$_2$ interface

region relative to the free surfaces. This important behavior even in such an idealized interface is because of the fact that the interface Si and Hf atoms are adequately passivated by the O atoms, resulting in species in their nominal oxidation states (as indicated by a Mulliken charge analysis) and with lower polarizability than the ones at the free surfaces.
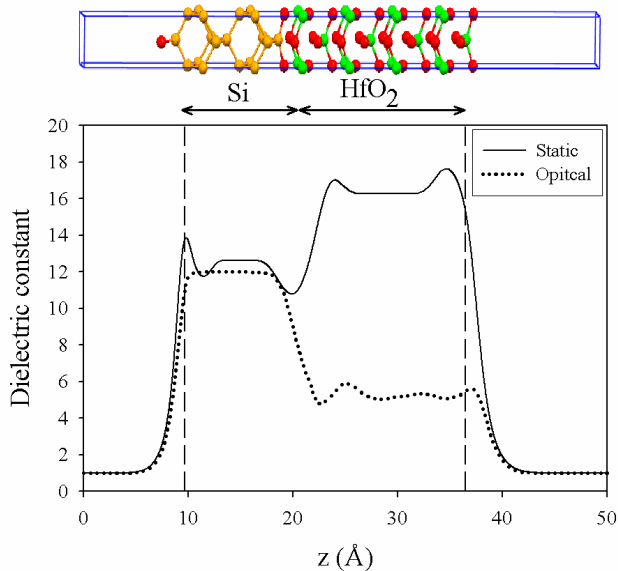
Figure 2. Above: Atomic model of Si-HfO$_2$ interface with O termination, with Si shown in gold, O in red, and Hf in green. Below: Static (solid) and optical (dotted) dielectric constant of (001) Si-HfO$_2$ interface as a function of position z normal to the interface.

3.3 SiO$_2$-POLYMER INTERFACE

Polymeric systems constitute an important class of materials for capacitor and insulation technologies [48]. Nevertheless, a quantitative understanding of the electrical response of such systems is still lacking [48, 49]. Polymer-nanocomposites, which have shown promise for electrical applications, form a class of systems that are even less understood. In this section and in Section 4.3, we investigate the dielectric and electronic properties at model polymer-silica interfaces.

Nanocomposites made by blending oxide nanoparticles with polymers are known to display higher effective permittivities than expected from the permittivities of the components, indicating the role played by enhanced interfacial polarization [4-7]. Here, we explore factors that could result in such permittivity enhancements in polymeric systems.

The SiO$_2$-polymer interface system considered here is composed of SiO$_2$ in the α-quartz phase of thickness 15.96 Å, and the polymer chain was approximated by a C$_{12}$H$_{26}$ molecule. Figure 3 shows the dielectric constant as a function of position along the SiO$_2$-polymer interface normal. Similar behavior of dielectric constant is observed as with the Si–SiO$_2$ interface. The agreement is excellent for the dielectric constant in the interior region of SiO$_2$ and polymer (C$_{12}$H$_{26}$) with the corresponding experimental single component bulk values, and the dielectric constant on the SiO$_2$ side of the interface is enhanced. Analysis of the Mulliken charges of the atoms indicates that C atoms closest to the interface are in

their nominal oxidation states (i.e., in oxidation states similar to that of C atoms in the interior of the polymer chain), whereas the Si and O atoms close to the interface are in varying oxidation states similar to that in the Si–SiO$_2$ case [20].

Our conclusion of permittivity enhancement at the interface is thus consistent with some prior experimental work [7]. Nevertheless, an *important* point needs to be made. The SiO$_2$-polymer system modeled here corresponds to a situation in which the SiO$_2$ surface is "untreated" (which is the experimental situation involving "blends" as in Ref. [7]). However, typical polymeric nanocomposites are made using silane-treated SiO$_2$ [50-53]. Silane treatment accomplishes the twin purposes of passivation of dangling bonds on silica surfaces by the silane-based initiator molecules, and in the creation of chemical bonds between the initiator and the polymer chains. Thus, silane treatment is expected to *decrease* the polarizability and permittivity at the interface. In fact, recent experimental work indicates that the incorporation of silane-treated SiO$_2$ nanoparticles into polyethylene results in decreased effective permittivities (although the permittivity of SiO$_2$ is *higher* than that of the host polymer) [50]. A more comprehensive analysis of SiO$_2$-polymer interfaces is necessary to understand the circumstances that would result in a permittivity increase or decrease at the interface.

Incidentally, incorporation of silane-treated SiO$_2$ nanoparticles into polyethylene also resulted in *increased* dielectric breakdown strength [50], while incorporation of micron-sized particles did not. It thus appears that the interface between SiO$_2$ and polyethylene plays a critical role in controlling the dielectric constant as well as the dielectric strength. These issues are explored further in Section 4.3.

It is worth mentioning that although we have studied only coherent interfaces between dissimilar materials, our approach to computing the local polarization and permittivity can be used to systematically explore a variety of realistic situations, including atomic-level defects (e.g., vacancies), disorder, impurities and initiator species at the interface.
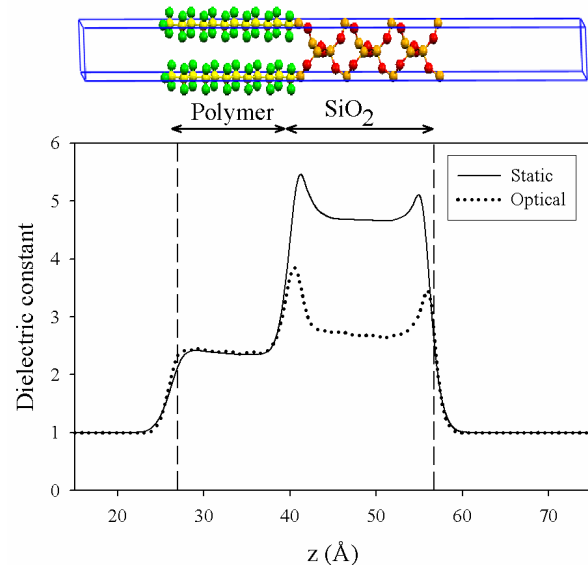
Figure 3. Above: Atomic model of SiO$_2$-polymer, with Si shown in gold, O in red, C in yellow, and H in green. Below: Static (solid) and optical (dotted) dielectric constant of C$_{12}$H$_{25}$-SiO$_2$ stack as a function of position z normal to the interface.

4 THE *LOCAL* ELECTRONIC STRUCTURE

At the surface of an insulating material or at the interface between two otherwise defect-free insulators, one generally finds under-coordinated atoms. These sub-optimal bonding situations lead to unoccupied and/or occupied states within the band gap of the insulators, which are localized physically at the surface or interface (as opposed to the delocalized bulk Bloch states), and are generally referred to as surface/interface states, defect states, or "trap" states. Reviews of these general notions can be found elsewhere [54, 55]. These defect states are important in two respects. They can alter the polarizability of the surface/interface region, as has been discussed in the previous section, and they can significantly control charge carrier conduction through the insulator. It is the latter possibility that is important in a study of breakdown phenomena.

In the case of *coherent* interfaces between dissimilar insulators, no dangling bonds would exist, and hence, one would not find defect states at the interface. Nevertheless, the energetic positions of the conduction and valence band edges in one material will be offset relative to those of the other material. In addition, the band edges could vary with position resulting in band bending due to transfer of charge from one material to the other at the interface.

It is important to characterize both the band offsets across the interface and the existence of trap states at the interface. Below, we present an approach to study the position dependent variation of the valence and conduction bands across interfaces, and the emergence of trap states at interfaces, using the layer-decomposed density of states (LaDOS) method. We then apply this method to Si-HfO$_2$ and polymer-SiO$_2$ interfaces.

4.1 THEORY (LaDOS)

Within the layer-decomposed density of states (LaDOS) approach, the total density of states (DOS) of the entire system is decomposed in terms of its origins from the various atoms of the system on a layer-by-layer basis. Since we are primarily interested in multi-layered systems, the layer decomposition provides the position dependence of the electronic structure that we seek.

Within a local orbital implementation of DFT such as the one adopted here, the electronic wave function $|\Psi_i\rangle$ can be projected onto the atomic orbitals $|\varphi_{al}\rangle$ as

$$| \Psi_i \rangle = \sum_{al} \langle \phi_{al} | \Psi_i \rangle | \phi_{al} \rangle \qquad (5)$$

where i, a, and l are the indices for the electronic wave function, atom, and the atomic orbital, respectively. The density of states $g_{al}(\varepsilon)$, where ε is the electronic energy, arising from a specific atom a with atomic orbital l can be defined as:

$$g_{al}(\varepsilon) = \sum_i \left| \langle \phi_{al} | \Psi_i \rangle \right|^2 \delta(\varepsilon - \varepsilon_i) \qquad (6)$$

where δ represents the Dirac delta function.

The contribution of all the atomic orbitals in one specific atomic layer results in the LaDOS of that layer. As will be demonstrated in the examples below, the LaDOS approach provides significantly more detailed information than the conventional "bulk plus band lineup" method [58, 59] for determining band offsets at interfaces.

4.2 Si-HfO$_2$ INTERFACE

Since HfO$_2$ is considered as a promising replacement for SiO$_2$, a comprehensive investigation of the band profile, band gap variation and band alignment evolution as a function of interfacial bonding with Si is urgently needed [58-61].

Our model of a coherent Si-HfO$_2$ heterojunction has been described in Section 3.2. The top part of Figure 4 shows the atomic structure of the Si-HfO$_2$ heterojunction, with dot-dashed rectangular boxes defining each layer. The LaDOS profile corresponding to each layer is displayed in the bottom part of Figure 4, with the valence and conduction bands shown in black and blue, respectively. The LaDOS for layers in the interior region of the Si are essentially same, resulting in a uniform band gap of about 0.45 eV, which compares well with the DFT-LDA band gap of bulk silicon determined by others [62]. Similarly, we obtain a uniform band edge profile in the interior region of HfO$_2$, and a band gap value of about 4.5 eV, which also compares well with previous DFT-LDA estimates of the HfO$_2$ band gap [59, 63]. Note that the computed band gaps are underestimated relative to experimental values, consistent with the well known deficiency of DFT-LDA.

Close to the Si-HfO$_2$ interface, the band edges of one system smoothly evolve to those of the other, resulting in a valence band offset of 3.05 eV between Si and HfO$_2$. This result compares well with the experimental estimates of 2.94-3.25 eV [59-61] and earlier calculations [58, 59] based on more involved computational treatments. Although LDA tends to underestimate band gaps of insulators relative to experiments, the valence band offsets are generally reproduced accurately. The smooth evolution of the band edges across the interface, and the absence of interfacial defect states is a result of the coherent nature of this interface (which contains no dangling bonds).

A deeper (and more realistic) analysis of this band edge variation dependence on the interfacial bonding and interfacial phases might provide very useful information concerning this important class of systems.
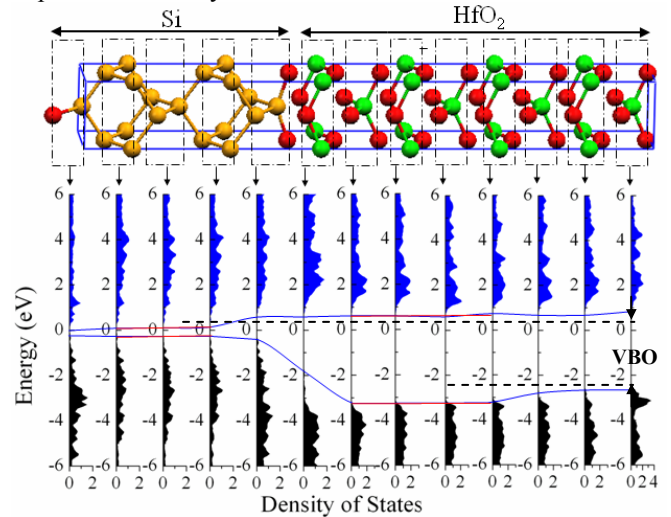
Figure 4. Above: Atomic model of Si-HfO$_2$ interface with O termination, with Si shown in gold, O in red, and Hf in green. Below: Layer-decomposed Density of States of Si-HfO$_2$ interface. The conduction band is shown in green, and the valence band in black. The zero of energy is the Fermi energy. The valence band offset (VBO) between Si and HfO$_2$ is determined to be 3.05 eV.

4.3 SiO$_2$-POLYMER INTERFACE

As mentioned in Section 3.3, recent experiments involving silane-treated SiO$_2$ nanoparticles incorporated in polyethylene has shown an increase in dielectric breakdown strength, whereas untreated SiO$_2$ displays only a modest change in the breakdown strength [50, 51]. It has also been postulated that interface states could act as potential electron traps, thereby scavenging "hot" electrons, and increasing the breakdown strength [56,57]. A systematic investigation of the various types of oxide-polymer interfaces focusing on interface states will help identify trends related to dielectric breakdown strengths, and can aid in the rational design of polymeric systems with superior dielectric properties.

In order to probe the specific role played by the silane treatment of SiO$_2$, we consider models of SiO$_2$-polymer interfaces in the presence of a silane-based species at the interface. The chemical route to the incorporation of silane-treated SiO$_2$ nanoparticles into the polymer involves two separate steps [50]. The SiO$_2$ nanoparticles are first reacted with silane or its derivatives, resulting in SiO$_2$ surfaces decorated with the silane-based initiator species. Next, the facile attachment of polymer chains to the initiator species is accomplished. In this work, the initiator is represented by a vinylsilanediol (HSi(OH)$_2$CHCH$_2$) molecule, and the polymer chain is C$_6$H$_7$F$_7$, representing polyvinylidene difluoride (PVDF). We find that attachment of the vinylsilanediol initiator to the SiO$_2$ surface (with a binding energy of -0.58 eV) and the subsequent attachment of C$_6$H$_7$F$_7$ to the initiator (with a binding energy of -0.98 eV) are thermodynamically favored.

The band edge variation with position perpendicular to the SiO$_2$ surface for a SiO$_2$-vinylsilanediol-PVDF interface is shown in Figure 5. The LaDOS in the middle parts of the SiO$_2$ and polymer regions result in a large and uniform band gaps, like in the coherent Si-HfO$_2$ example discussed above. However, in the interface region that contains the initiator, the band edges do not smoothly evolve from one region to the other. Rather, two peaks, one corresponding to an occupied defect state and another to an unoccupied defect state appear (indicated by circles in Figures 5), whose origins can be traced to the double bond in the vinylsilanediol initiator. Both the unoccupied and occupied states can be classified as "shallow" traps for electrons and holes, respectively, as they are close to the conduction band and valence band edges. These defect states are localized, and could potentially trap itinerant conduction electrons and valence holes, thereby providing opportunities for "cooling" charge carriers.

Although these aspects are consistent with the observed increase in breakdown strength of SiO$_2$-polymer composites, several questions remain unanswered. Firstly, mechanisms for the dissipation of the energy released during the cooling process need to be addressed. A potential mechanism could be the enhanced interaction between electrons in the polymer and phonons in SiO$_2$. It is well known that enhanced electron-phonon coupling in SiO$_2$ is one of the reasons for its high breakdown strength [55-56]. Secondly, the role of the initiator species needs to be clarified, as the trap states appear to be determined largely by the nature of the initiator. Thirdly, a
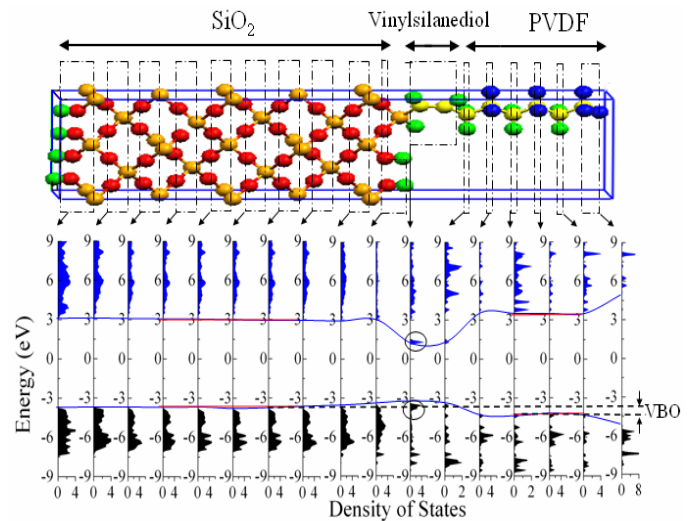
Figure 5. Above: Atomic model of SiO$_2$-vinylsilanediol-PVDF inter-face, SiO$_2$ slab with OH termination, with Si shown in gold, C in yellow, O in red, H in green, and F in blue. Below: Layer–decomposed Density of States of SiO$_2$-vinlysilanediol-PVDF interface. The conduction band is shown in blue, and the valence band in black. The zero of energy is the Fermi energy. Lower and upper circled states represent occupied and unoccupied interfacial defect states, respectively.

variety of SiO$_2$ and other oxide (e.g., Al$_2$O$_3$) surfaces should be studied to understand systematic trends across a wider class of situations. The LaDOS approach provides a practical framework to undertake such systematic studies.

5 SUMMARY

As component sizes or dimensions in multiple-component dielectric materials shrink to the atomic or nanoscale, the structure and chemistry at interfaces become important. Understanding the fundamental relationships between the atomic level interfacial structure and electrical properties such as dielectric response and breakdown is critical. In this work, we have presented two *ab initio* based computational methodologies to probe such structure-property relationships in systems of emerging technological importance.

The theory of the local dielectric permittivity has been developed to understand the variations of the static and optical dielectric constant across idealized Si-SiO$_2$, Si-HfO$_2$ and SiO$_2$-polymer interfaces over length scales of the order of interatomic distances. These variations have been correlated to the chemistry at the interfaces, such as dangling bonds and multiple oxidation states. The layer-decomposed density of states approach has been used to compute the electronic structure variation across Si-HfO$_2$ and SiO$_2$-polymer interfaces. This procedure has been used to capture band bending, band offsets and creation of trap states at interfaces. Although further work over a wider range of systems and situations is necessary, the computational tools and their applications described here form the groundwork for a more thorough analysis of the impact of surfaces, interfaces, and atomic level defects on the dielectric and electronic properties of a wide variety of nanostructured systems.

ACKNOWLEDGMENT

REFERENCES

[1]   G. D. Wilk, R. M. Wallece, and J. M. Anthony, "High-k gate dielectrics: Current status and materials properties considerations", J. Appl. Phys., Vol. 89, pp. 5243-5275, 2001.

[2]   A. I. Kingon, J. P. Maria, and S. K. Steiffer, "Alternative Dielectrics to Silicon Dioxide for Memory and Logic Devices", Nature (London), Vol. 406, pp. 1032-1038, 2000.

[3]   R. C. Advincula, "Surface initiated polymerization from nanoparticle surfaces", J. Dispersion Sci. Technol., Vol. 24, pp. 343-361, 2003.

[4]   S. S. Ray and M. Okamoto, "Polymer/layered silicate nano-composites: a review from preparation to processing", Prog. Polym. Sci., Vol. 28, pp. 1539-1641, 2003.

[5]   Y. Rao, and C. P. Wong, "Material characterization of a high-dielectric-constant polymer-ceramic composite for embedded capacitor for RF applications", J. Appl. Polym. Sci., Vol. 92, pp. 2228-2231, 2004.

[6]   S. OBrian, L. Brus, and C. B. Murray, "Synthesis of Monodisperse Nanoparticles of Barium Titanate: Toward a Generalized Strategy of Oxide Nanoparticle Synthesis", J. Am. Chem. Soc., Vol. 123, pp. 12085-12086, 2001.

[7]   P. Murugaraj, D. Mainwaring, and N. Mora-Huertas, "Dielectric enhancement in polymer-nanoparticle composites through interphase polarizability", J. Appl.   Phys., Vol. 98, pp. 054304 - 054309, 2005.

[8]   Q. M. Zhang, H. Li, M. Poh, F. Xia, Z.-Y. Cheng, H. Xu, and C. Huang, "An All-Organic Composite Actuator Materials with a High Dielectric Constant", Nature (London), Vol. 419, pp. 284-287, 2002.

[9]   M. L. Green, E. P. Gusev, R. Degreave, and E. L. Garfunkel, "Ultrathin (<4 nm) SiO_2 and Si-O-N gate dielectric layers for silicon microelectronics: Understanding the processing, structure, and physical and electrical limits", J. Appl. Phys., Vol. 90, p. 2057-2121, 2001.

[10] J. Robertson, "Interfaces and defects of high-k oxides on silicon", Solid-State Electronics, Vol. 49, pp. 283-293, 2005.

[11] K. Xiong and J. Robertson, M. C. Gibson and S. J. Clark, "Defect energy levels in HfO_2 high-dielectric-constant gate oxide", Appl. Phys. Lett. 87, pp. 183505-183507, 2005.

[12] K. Xiong and J. Robertson, S. J. Clark, "Defect states in the high-dielectric-constant gate oxide $LaAlO_3$", Appl. Phys. Lett., Vol. 89, pp. 022907-022909, 2006.

[13] R. Martin, *Electronic Structure: Basic Theory and Practical Methods*, Cambridge University Press, New York, 2004.

[14] J. M. Soler, E. Artacho, J. Gale, A. Garcia, J. Junquera, P. Ordejon, and D. Sanchez-Portal, "The SIESTA method for *ab initio* order-*N* materials simulation", J. Phys.: Condens. Matter, Vol. 14, pp. 2745-2779, 2002.

[15] F. Giustino and A. Pasquarello, "Theory of atomic-scale dielectric permittivity at insulator interfaces", Phys. Rev. B, Vol. 71, pp. 144104 - 144116, 2005.

[16] F. Giustino, P. Umari, and A. Pasquarello, "Dielectric Discontinuity at Interfaces in the Atomic-Scale Limit: Permittivity of Ultrathin Oxide Films on Silicon", Phys. Rev. Lett., Vol. 91, pp. 267601-267604, 2003.

[17] Data collected by C. Kittel, in *Introdunction to Solid State Physics,* 5th ed, Wiley, New York, 1976 and references therein.

[18] F. Liu, S. H. Garofalini, D. Kingsmith, and D. Vanderbilt, "First-principles study of crystalline silica", Phys. Rev. B, Vol. 49, pp. 12528-12534, 1994.

[19] N. R. Keskar and J. R. Chelikowsky, "Structural properties of nine silica polymorphs", Phys. Rev. B, Vol. 46, pp. 1-14, 1992.

[20] L. Levien, C. T. Prewitt, and D. J. Weidner, "Structure and elastic properties of quartz at pressure", Am. Mineral., Vol. 65, pp. 920-930, 1980.

[21] N. Tit and M. W. C. Dharma-Wardana, "Electronic states and optical properties of Si/SiO_2 superlattices", J. Appl. Phys., Vol. 86, pp. 387-395, 1999.

[22] R. W. G. Wyckoff, *Crystal Structure*, 4th ed. Interscience, New York, 1974, and references therein.

[23] Xinyuan Zhao and David Vanderbilt, "First-principles study of structural, vibrational, and lattice dielectric properties of hafnium oxide", Phys. Rev. B, Vol. 65, pp. 233106 – 233109, 2002.

[24] A. A. Demkov, "Investigating Alternative Gate Dielectrics: A Theoretical Approach", Phys. Status Solidi B., Vol. 226, pp. 57–67, 2001.

[25] J. Wang, H. Li, and R. Stevens, "Hafnia and hafnia-toughened ceramics", J. Mater. Sci., vol. 27, pp. 5397 -5430, 1992.

[26] J. Adam and M. D. Rodgers, "The crystal structure of ZrO_2 and HfO_2", Acta Crystallogr., Vol., 12, pp. 951, 1959.

[27] Eabien Picaud, Alexander Smogunove, Andrea Dal Corso, and Erio Tosatti, "Complex band structures and decay length in polyethylene chains", J. Phys.: Condens. Matter, Vol. 15, pp. 3731-3740, 2003.

[28] M. Rubinstein and R. Colby, *Polymer Physics,* Oxford University, Press, New York, 2003.

[29] V. S. Bystrov, N. K. Bystrova, E. V. Paramonova, and A. V. Sapronova, "Computational Nanostructures and Physical properties of the Ultra-Thin ferroelectric langmuir-blodgett Films", Ferroelectric Letters, Vol.33, p. 153-162, 2006.

[30] D. Tulumello, G. Cooper, I. Koprinarov, and A. P. Hitchcock, "Inner-Shell Excitation Spectroscopy and X-ray Photoemission Electron Microscopy of Adhesion Promoters", J. Phys. Chem. B, Vol 109, pp. 6343-6354, 2005.

[31] R. Ramprasad and N. Shi, "Dielectric properties of nanoscale HfO_2 slabs", Phys. Rev. B, Vol. 72, pp. 052107 – 052110, 2005.

[32] N. Shi and R. Ramprasad, "Dielectric properties of ultrathin SiO_2 slabs", Appl. Phys. Lett., Vol. 87, pp. 262102 – 262104, 2005.

[33] X. Zhao and D.Vanderbilt, "Phonons and lattice dielectric properties of zirconia", Phys. Rev. B, Vol. 65, pp. 075105 – 075114, 2002.

[34] S. Sayan, N.V. Nguyen, J. Ehrstein, T. Emge, E. Garfunkel, M. Croft, Xinyuan Zhao, David Vanderbilt, I. Levin, E. P. Gusev, Hyoungsub Kim, and P. J. McIntyre, "Structural, electronic, and dielectric properties of ultrathin zirconia films on silicon", Appl. Phys. Lett., Vol. 86, pp. 152902-152904, 2005.

[35] N. Shi and R. Ramprasad, "Atomic-scale dielectric permittivity profiles in slabs and multilayers", Phys. Rev. B, Vol. 74, pp. 045318 – 045321, 2006.

[36] N. Shi and R. Ramprasad, "Dielectric properties of nanoscale multi-component systems: A first principles computational study", J. Computer-Aided Materials Design, Vol. 10820, pp.133-139, 2006.

[37] J. D. Jackson, *Classical Electrodynamics,* University of California, Berkeley, 1998.

[38] D. A. Buchanan, "Scaling the gate dielectric: Materials, integration, and reliability", IBM J. Res. Dev. 43, 245-264, 1999.

[39] C. A. Balans, *Advanced Engineering Electromagnetics* , Arizona State University, New York, 1989.

[40] L. E. Ramos, J. Furthmuller, and F. Bechstedt, "Quasiparticle band structures and optical spectra of β-cristobalite SiO_2" , Phys. Rev. B, Vol. 69, pp. 085102 -085109, 2004.

[41] W. G. Wolf, S. B. Stanley, and K. A. McCarthy, *American Instituteof Physics Handbook,* McGraw-Hill, New York, 1963, p.24.

[42] H.S. Chang, H. D. Yang, and H. Hwang, "Measurement of the physical and electrical thickness of ultrathin gate oxides", J. Vac. Sci. Technol. B, Vol. 20, pp. 1836-1842, 2002.

[43] V. Fiorentini and G. Gulleri, "Theoretical Evaluation of Zirconia and Hafnia as Gate Oxides for Si Microelectronics", Phys. Rev. Lett., Vol. 89, pp. 266101-266104, 2002.

[44] P. W. Peacock, K. Xiong, K. Y. Tse, and J. Robertson, "Bonding and interface states of Si:HfO_2 and Si:ZrO_2 interfaces", Phys. Rev. B, Vol. 73, pp. 075328- 075339, 2006.

[45] E. Cockayne, "Influence of oxygen vacancies on the dielectric properties of hafnia: First-principles calculations", Phys. Rev. B., Vol. 75, pp. 094103-094110, 2007.

[46] R. K. Nahar, V. Singh and A. Sharma, "Study of electrical and microstructure properties of high dielectric hafnium oxide thin film for MOS", J. Mater. Sci.: Mater Electron, Vol. 18, pp. 615-619, 2007.

[47] G.-M. Rignanese, X. Gonze, G. Jun, K. Cho and A. Pasquarello, "First-principles investigation of high-k dielectrics: Comparison between the silicates and oxides of hafnium and zirconium", Phys. Rev. B, Vol. 69, pp. 184301-184310, 2004.

[48] S .Boggs, "Very high field phenomena in dielectrics", IEEE Trans. Dielectr. Electr. Insul., Vol. 12, pp. 929-938, 2005.

[49] G. Teyssedre and C. Laurent, "Charge transport modeling in insulating polymers: form molecular to macroscopic scale", IEEE Trans. Dielectr. Electr. Insul., Vol. 12, pp. 857-875, 2005.

[50] M. Roy, J. K. Nelson, R. K. MacCrone, L. S. Schadler, C. W. Reed, R. Keefe and W. Zenger, "Polymer nanocomposite dielectrics – the role of the interface", IEEE Trans. Dielectr. Electr. Insul., Vol. 12, pp. 629- 43 and pp. 1273, 2005.

[51] J. Keith Nelson, "The promise of Dielectric Nanocomposites", IEEE Intern. Sympos. Electr. Insul. (ISEI), pp. 452-457, 2006.

[52] Y. Cao, P. C. Irwin and K. Younsi, "The Future of Nanodielectrics in the Electrical Power Industry", IEEE Trans. Dielectr. Electr. Insul., Vol. 11, pp. 797-807, 2004.

[53] M. Kaufhold, K. Schafer, K. Bauer, A. Bethge and J. Risse, "Interface Phenomena in Stator Winding Insulation - Challenges in Design, Diagnosis, and Service Experience", IEEE Electr. Insul. Mag., Vol. 18, No.2, pp. 27-36, 2002.

[54] C. Kittel, *Introduction to Solid State Physics*, 2^{ed}, John Wiley & Sons. Inc, New York, 1963.

[55] J. Callaway, *Energy Band theory*, Academic Press Inc., New York, 1964.

[56] T. H. DiStefano and M. Shatzkes, "Impact ionization model for dielectric instability and breakdown", Appl. Phys. Lett. , Vol. 25, pp. 685-687, 1974.

[57] Z. Chen, J. Guo and F.Q. Yang, "Phonon-energy-coupling enhancement: Strengthening the chemical bonds of the SiO_2/Si system", Appl. Phys. Lett., Vol. 88, pp. 082905 -082907, 2006.

[58] S. Sayan, T. Emge, E. Garfunkel, X. Zhao, L. Wielunski, R. Bartynski,D. Vanderbilt, J. Suehle, S. Suzer, and M. Banaszak-Holl, "Band alignment issues related to $HfO_2/SiO_2/p$-Si gate stacks", J. Appl. Phys. ,Vol. 96, pp.7485-7491, 2004.

[59] B. R. Tuttle, C. Tang and R. Ramprasad, "First-principles study of the valence band offset between silicon and hafnia", Phys. Rev. B, Vol. 75, in print, 2007.

.

[60] M. Oshima, S. Toyoda, T. Okumura, J. Okabayashi, H. Kumigashira, K. Ono, M. Niwa, K. Usuda, and N. Hirashita, "Chemistry and band offsets of HfO_2 thin films for gate insulators", Appl. Phys. Lett., Vol. 83, pp. 2172-2174, 2003.

[61] O. Renault, N. T. Barrett, D. Samour, and S. Quiais-Marthon, "Electronics of the SiO_2/HfO_2 interface by soft X-ray photoemission spectroscopy", Surf. Sci. Vol. 566, pp. 526-531, 2004.

[62] P. E. Van camp, V. E. Van Doren, and J. T. Devreese, "First-principles calculation of the pressure coefficient of the indirect bang gap and the charge density of C and Si", Phys. Rev. B., Vol.34, pp. 1314-1317, 1986.

[63] J. E. Jaffe, R. A. Bachorz, and M. Gutowski, "Low-temperature polymorphs of ZrO_2 and HfO_2: A density-functional theory study", Phys. Rev. B, Vol. 72, pp. 144107-144115, 2005.

Ning Shi graduated from Nanjing University of Sci. and Tech., China, with B.S. and M.S. degrees in physical electronics. She is presently a graduate student in the department of Chemical, Materials, and Biomolecular Engineering at the University of Connecticut.

Ramamurthy Ramprasad graduated from the Indian Institute of Technology, Madras, India, in 1990 with a B.Tech. degree in metallurgical engineering, and from the University of Illinois, Urbana-Champaign, in 1997 with a Ph.D. degree in materials science and engineering. After a six-year stint at Motorola, Inc., where he worked on problems related to field emission for flat panel display applications, advanced dielectric and magnetic materials, and metamaterials for RF and microwave applications, he joined the Department of Materials Science & Engineering at the University of Connecticut as a faculty member. His current research is focused on developing and applying modern electronic structure computational methods to nanostructured systems containing interfaces. Dr. Ramprasad is the author of about 40 peer-reviewed journal papers, numerous conference papers, and 4 patents